The Seventh Asian-Pacific Symposium on Structural Reliability and Its Applications (APSSRA2020)
October 4–7 2020, Tokyo, Japan
T. Takada, I. Yoshida & T. Itoi (editors)

Risk-informed Landslide Hazard Mitigation in Mountain Highway Design

Li-Min Zhang[1], Rui-Lin Fan[2] and Te Xiao[3]

[1]*The Hong Kong University of Science and Technology, Clear Water Bay, Hong Kong. Email: cezhangl@ust.hk*
[2]*The Hong Kong University of Science and Technology, Clear Water Bay, Hong Kong. Email: rfanaa@connect.ust.hk*
[3]*The Hong Kong University of Science and Technology, Clear Water Bay, Hong Kong. Email: xiaote@ust.hk*

Abstract: This paper presents the methodology and outcome of a novel quantitative risk assessment implemented in a 10-year reconstruction project of two mountain highways in the epicenter area of the 2008 Wenchuan earthquake. Routed in deep valleys, the highways were severely damaged during and on multiple counts after the earthquake, making highway reconstruction life-threatening. After the earthquake, the highways were initially covered by loose soil deposits of landslides, and subsequently exposed to frequent landslide hazard chains in the forms of rock falls, rain-induced landslides, debris flows, landslide damming and flooding. The success of the reconstruction projects depends on the degree of landslide risk mitigation, which this paper defines as individual risk and potential loss of life. The paper describes how risk-informed decisions were made in the design and selection of highway alignment options and engineering risk mitigation measures, which were tested by a quantitative risk assessment procedure. Significant efforts were made to understand landslide hazard chains along the highways, particularly interactions between separate hazards in each chain, and their evolution over time. The quantitative risk assessment resulted in a significant reduction (to about 20% and 33% of the initial risk levels for Highways S303 and G213, respectively) in potential loss of life through the use of long tunnels to bypass the high-risk landslide zones and protective measures which respond more effectively to manageable, smaller scale hazards. Today, the approach of this study has influenced and become routine practice in the design and construction of new highways in the seismic mountainous region of western China.

Keywords: landslide, risk assessment, decision, highway, earthquake.

1. Co-seismic Landslides and Damages to Highways in the Epicenter Area of the Wenchuan Earthquake

The Ms 8.0 Wenchuan earthquake on 12 May 2008 occurred on the eastern margin of the Qinghai-Tibet plateau. This area is featured by rugged terrains due to significant uplift from tectonic movements and deep cuts by large rivers. During the earthquake, strong ground motions caused more than 60,000 large-scale landslides over an area of 35,000 km^2 (e.g. Huang and Fan, 2013). Figure 1 shows the landslides in the epicentral area near Yingxiu Town, Sichuan Province, China. Approximately 30% of the land surface was covered by landslide soil deposits shortly after the earthquake. Two rivers, the Minjiang River and the Yuzixi River, meet at Yingxiu Town, forming steep terrains and deep valleys with elevations varying from 870 m at Yingxiu to 4083 m at the mountain top and an internal relief of over 3200 m.

Two major highways are routed along the rivers: National Highway G213 along the Minjiang River and State Highway S303 along the Yuzixi River. Many bridge structures along the highways were destroyed by earthquake-induced landslides (Figure 2). More devastating damage to the highways was caused by the extensive landslides that buried more than half of S303 between Yingxiu and Gengda aligned along the Yuzixi River (Figure 3).

Zhang et al. (2014b) mapped the co-seismic landslides in an 85 km^2 area along S303 from milestone K1 to K18, located exactly between Yingxiu where the Yingxiu-Beichuan Fault is located, and Gengda where the Maoxian-Wenchuan Fault is located (Figure 1). The lithology in this area mainly consists of medium fine-grained granite, diorite and alluvium. A total of 305 hillslope shallow slides were identified (Figure 4) in this area. The slope gradients of these 305 loose deposits

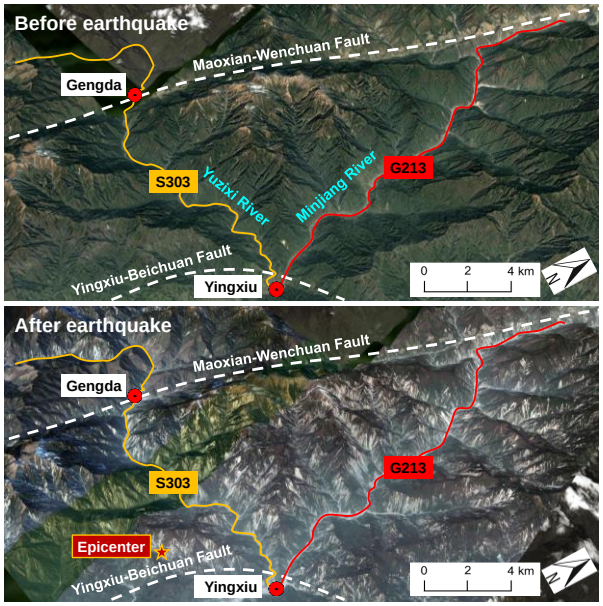

Figure 1. Landslides near the epicenter of the Wenchuan earthquake in May 2008.

Figure 2. Damage to bridges due to landslides.

Figure 3. Burial of Highway S303 along the Yuzixi River.

range from 6 ° to 54 °. The landslides cover a total area of 24.02 km^2 (28.3%) and have a total volume of 54.3×10^6 m^3. Figure 5 shows the distributions of altitude and internal relief of these landslides. Approximately 83% of the earthquake-induced landslides were located in areas with internal relief between 400 m and 1600 m, higher than the landslides in the rest parts of the Wenchuan earthquake zone. In addition, a total of 28 channel deposits were identified, which are distributed in various catchments and have a total volume of 12.39×10^6 m^3.

2. Need for Systematic Landslide Risk Assessment

Highway reconstruction after strong earthquakes has long been challenging worldwide. The reconstruction of G213 and S303 starting from the epicenter of the Wenchuan earthquake, in particular, is unprecedented considering the record high landslide density (Figure 1), deep valley terrain, and active, post-earthquake cascading landslides.

G213 is the only major highway from Chengdu to Wenchuan and western Sichuan; hence it was required to implement a temporary access road along its original route before the end of August 2008, then reconstruct this 53.3 km Yingxiu-Wenchuan highway over a period of 3 years. Similarly, the reconstruction of the 45 km Yingxiu-Wolong highway (S303) started in April 2009 and was scheduled to complete in 3 years. By early August 2010, the roadbed of S303 had largely been

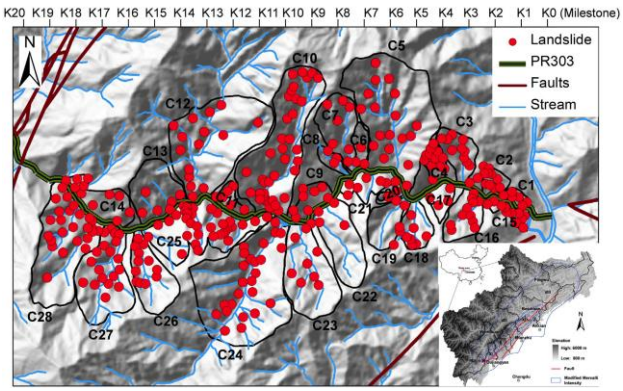

Figure 4. Distribution of 305 loose deposits between K1 and K18 along S303.

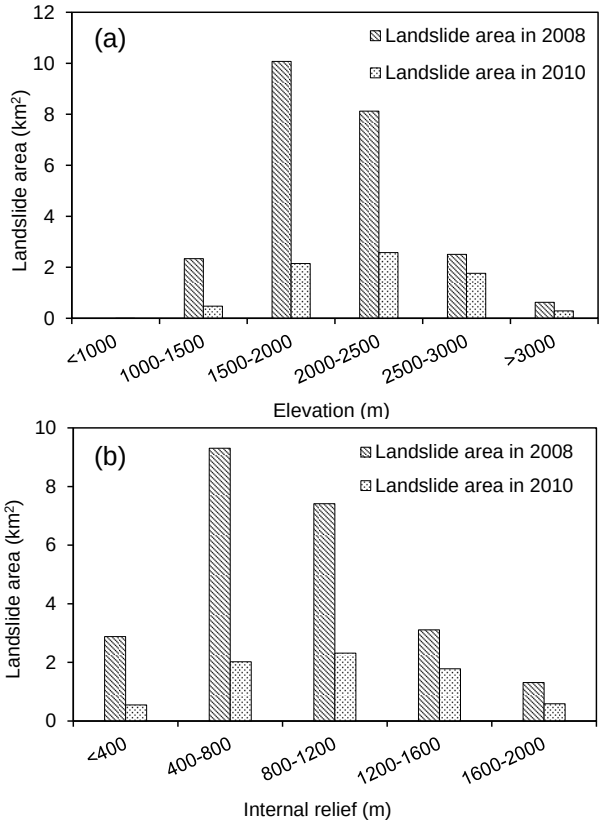

Figure 5. Distributions of (a) altitude and (b) internal relief of the co-seismic landslides along S303.

completed and partially paved. The two new highways were primarily constructed along their previous routes, with short tunnels occasionally to avoid excessive detours. Particular measures were taken to protect the highways against landslides, rock falls and debris flows based on the characterization of the landslide deposits seen shortly after the earthquake, given the uncertainty of cascading hazards in the following years. The hazard mitigation measures included shed tunnels, flexible barriers, gabions, and debris-flow diversion channels, etc.

Then came the first large rainstorm after the earthquake on 12-14 August 2010. A cumulative rainfall of 226 mm was recorded within 39 h from 17:00 on 12 August to 7:00 on 14 August. Particularly, a cumulative rainfall amount of 185 mm was recorded by about 4:00 am on 14 August 2010, when local residents witnessed widespread landslides and debris flows. A total of 351 fresh rain-induced landslides were identified along S303 (Figure 6), including 322 reactivated shallow landslides which occurred in the pre-existing landslide deposits induced in 2008, and 29 new landslides which occurred at locations not affected by the landslides in 2008. These landslides covered an area of 7.26 km^2. During the August 2010 storm, 12 channelized debris flows and 14 hillslope debris flows were also triggered along S303, covering an area of 2.68 km^2. Most of the new highway was buried again by the extensive rain-induced landslides and debris flows. In particular, the portal of the 1246 m long Nanhua Tunnel, which had just been completed in May 2010, was buried by the large debris flow at

Xiaojiagou (Chen et al., 2012). This debris flow also blocked the Yuzixi River, forming a landslide dam and a barrier lake that lifted the riverbed by more than 20 m and inundated a section of the highway. After the August 2010 storm, the highway authority turned the damaged highway into a temporary access road by bypassing the tunnel with a temporary detour along the river in the valley.

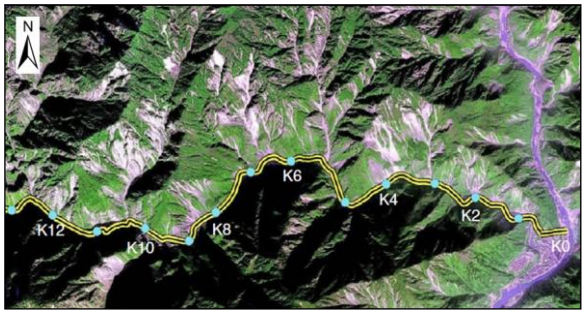

Figure 6. Landslides along S303 triggered by the 12-14 August 2010 rainstorm.

Similar to the storm in August 2010, the subsequent rainstorms continued to repetitively trigger a large number of landslides and debris flows in the area. The July 2011 storm triggered 157 fresh landslides alone. These fresh landslides included 133 reactivated shallow landslides and 24 new landslides at locations that had not failed in 2008. In July 2013, the number of fresh rain-induced landslides was 135. In each of the storms, the access road that was resumed after the wet season of the previous year was buried again by the widespread landslides and debris flows.

The resulting challenge was that post-seismic landslide hazards differed significantly from design scenarios assumed immediately post-earthquake, leading to frequent engineering failures, and the need to launch another round of reconstruction. The second round of S303 reconstruction started in July 2012. Comprehensive risk assessment was performed to assist the selection of the new highway alignment and risk mitigation measures. The project was successfully completed in October 2016. The design insights gained from the new design for S303 were applied to the new round of reconstruction of G213, which started in July 2015 and was completed in December 2018.

3. Multi-hazard Risk Assessment

In the new round of investigations and design, the first critical issue was to understand the landslide hazard chains in time and space, and to quantify the impact of such landslide hazard chains on the highways.

3.1 Hazard interactions in space and time

A large rainstorm can trigger numerous landslides and debris flows, which may interact with each other and trigger tertiary hazards such as landslide damming, dam breaching, and rising riverbeds, referred to as a landslide hazard chain (Fan et al., 2019). A summary of interactions among landslide hazards is as follows:

(1) Overlapping of several hazards of the same type. For example, the fans of two debris flows can overlap, and the impact areas of several slides or rock falls can also overlap. Such overlapping will affect both the destructive power of the hazards and the vulnerability to the hazards.
(2) Overlapping of influence zones of different types of hazards. During a severe storm, a particular area may be concurrently impacted by flooding, rain-induced landslides and debris flows. For instance, Beichuan Town suffered from seven episodes of hazards within a period of five years after the earthquake (i.e. 2008-2013) (Zhang et al., 2014a).
(3) Merging of numerous smaller debris flows of various origins into a larger debris flow, such as the debris flows at Gaojiagou nearby G213 under the 1-3 July 2011 storm (Fan et al., 2018).
(4) Domino effects or cascading landslides, in which an initiating event causes a chain of disaster events, with the outcome of one event being the cause of other events. A storm triggered numerous soil slides and debris flows. Some of the slide materials turned into debris flows. The combined debris flow ran into a river and blocked the river, forming a landslide dam and inundating a stretch of highway in the landslide lake. The subsequent dam breaching flood may cause severe scouring of the downstream roadbed.

During the evolution of the landslide hazards, their impact on the highways also evolved over time (Zhang et al., 2016), as shown in Figure 7. Shortly after the earthquake, rock falls and flying rocks were the most dangerous for highway users in the deep valleys. Later, amidst heavy storms, rain-induced landslides and debris flows became the most damaging. Since 2012, as the riverbed rose significantly due to the excessive discharge of sediment and debris flow materials into the river system, the river water level in summer reached the road level and scour-related hazard become a major issue. The riverbed elevation eventually rose to match the invert elevation of the Bauhinia Tunnel, the longest tunnel of S303, such that this tunnel was abandoned eventually.

Figure 7. Evolution of earthquake-induced landslide hazards over time: (a) landslide; (b) debris flow; (c) dam breach; (d) uplifted riverbed; (e) dam breach; (f) uplifted riverbed.

3.2 Quantitative risk assessment

Lacasse and Nadim (2009) and many others presented the latest methodologies for the assessment, mitigation and management of landslide risk. Recently Zhang (2014) and Zhang et al. (2014a) proposed a quantitative framework of multi-hazard risk assessment to evaluate the risks posed by cascading landslide hazards considering the interactions among various hazards and the possible cascading effects on human vulnerability. Attention was paid to the quantification of the amplification and overlapping effects due to the interactions among two or more hazards. The framework consists of five phases, including definition, multi-hazard assessment, exposure assessment, multi-vulnerability assessment, and multi- risk assessment:

(1) Definition of the time and space scales for hazard analysis, risk sources, and initiating events.
(2) Multi-hazard assessment, which includes identifying hazard scenarios and links between these scenarios, and quantifying their occurrence probabilities.
(3) Exposure assessment, which assesses the interactions between exposure elements and estimates the elements at risk considering the overlapping or amplification effects.
(4) Multi-vulnerability assessment, which quantifies the vulnerability of the elements at risk in each affected area to one or multiple hazards.
(5) Multi-risk assessment, in which the risk of the cascading hazards is expressed as the sum of all risks posed by these hazards, as well as new hazards derived from the hazard interactions, in a pre-defined area, as shown in Figure 8.

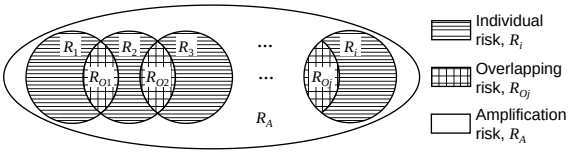

Figure 8. Multi-risk assessment in the five-phase framework.

Specifically, the procedure for rapid risk assessment of rain-induced landslide and debris flow hazards can be implemented in a cell-based platform step by step:

(1) Discretize the digital terrain of the study area into a grid, with properties for each cell assigned, such as geology, topography, soil properties, hydrological parameters, and groundwater table. Map rainfall from rain gauges to each cell using spatial interpolation techniques, such as Kriging.
(2) Given the spatiotemporal rainfall distribution, the runoff and rainfall infiltration processes can be analyzed, providing spatial and temporal pore-water pressure profiles of each cell. The stability and reliability of each cell, and the movement trace and deposition location of detached material from each unstable cell can then be assessed using a slope failure prediction module (e.g. Chen and Zhang, 2014; Chen et al., 2015). For example, a one-dimensional infinite slope model can be adopted for slope stability analysis as most natural terrain landslides are shallow failures and such a model is computationally efficient for large areas. Various uncertainties can be incorporated to evaluate the failure probability of each cell using reliability methods (e.g. first-order second-moment method, Monte Carlo simulation). A mass movement analysis is required to find the landslide path. In addition to physically based methods, empirical relationships can also be applied (e.g. Chen and Zhang, 2014). The vulnerability of the travelers in vehicles to slope failures can be indicated by the volume and angle of reach of the slope failure.
(3) The occurrence probability, volume and impacted area of the rainfall-induced debris flows can be obtained by a debris flow simulation model. Data-driven logistic regression analysis is widely adopted for computing the occurrence probability of debris flows in each catchment. The debris-flow runout behavior can be simulated physically using software such as EDDA (Chen and Zhang, 2015; Shen et al., 2018). The vulnerability of the travelers in vehicles to debris flows can be represented by the debris depth.
(4) Afterwards, the risks of slope failures and debris flows can be assessed by a quantitative multi-hazard risk assessment module, which will be introduced later in this paper. The contribution of rainfall-induced slope failures to debris flows and the scenario of a location impacted by multiple slope failures or debris flows, or both, can be properly accounted for in such a cell-based platform.

The risk is usually presented in two levels for different purposes, namely the societal risk to the whole population, independent of geographical location, and the individual risk to a single person at a specific location. Suppose there are n mutually exclusive landslide events. The societal risk, in terms of the annual potential loss of life (PLL), $R_{(PLL)}$, is defined as the sum of the products of the conditional temporary and spatial probabilities and the consequence caused by the individual loose deposits (Fell et al., 2005):

$$R_{(PLL)} = \sum_{i=1}^{n} [P_{(L)i} \times P_{(T:L)i} \times P_{(S:T)i}] \times [V_{(D:S)i} \times E_i] \quad (1)$$

where $P_{(L)i}$, $P_{(T:L)i}$ and $P_{(S:T)i}$ are the annual occurrence probability of landslide incident i, the probability of landslide incident i reaching the highway, and the probability that passengers are present at the location impacted by landslide incident i, respectively; $V_{(D:S)i}$ is the vulnerability of the passengers to landslide incident i (i.e. the chance of the passengers lose their lives when they are impacted by the landslide); E_i is the number of persons at risk by landslide incident i. The individual risk of loss of life, $R_{(DI)}$, is defined as (AGS, 2000):

$$R_{(DI)} = \sum_{i=1}^{n} P_{(L)i} \times P_{(T:L)i} \times P_{(S:T)i} \times V_{(D:S)i} \quad (2)$$

To facilitate assessing the risk profile of the highways, both the individual risk and societal risk are better to be expressed on an F-N curve, i.e. a graphical representation of the cumulative frequency of N or more fatalities (i.e. F) against the number of fatalities (i.e. N) on a log-log scale.

Given a triggering storm, the F-N curve, with respect to societal risk for example, can be generated in the following steps:

(1) Identify possible landslides and debris flows triggered by the storm.
(2) Determine the factor of safety and failure probability, $P_{(L)i}$, of each soil deposit.
(3) Perform travel analysis for landslides and debris flows to calculate runout distances and corresponding $P_{(T:L)i}$.
(4) Determine passenger behaviors to determine $P_{(S:T)i}$ and the vulnerability $V_{(D:S)i}$.
(5) Estimate elements at risk, E_i, in line with design traffic conditions.
(6) Evaluate the potential loss of life caused by each landslide.
(7) Rank the landslides according to their PLL values and calculate the cumulate frequency of N or more PLLs.
(8) Plot the F-N curve, with F being the cumulative frequency multiplied by the annual frequency of the triggering storm.

Various uncertainties that govern the landslide impact can be incorporated in a more rigorous Monte Carlo simulation framework, such as rainfall distributions, shear strength and seepage parameters that characterise slope stability and landslide volume; terrain and surface parameters that describe mass flow and runout distance of the landslide; and number, value and characteristics of elements at risk that determine the exposure of elements at risk and their vulnerability to the landslide. In this method, a number of realizations of uncertain parameters can be generated and an F-N curve can be produced for each realization using the aforementioned procedure, leading to a family of F-N curves that characterize the variability of a risk profile.

4. Risk-informed Engineering Decision for S303

The risk analysis procedure in the above section was applied to assist engineering design decisions in ranking the risks of hanging landslide soil deposits, selecting highway alignment, and choosing landslide risk mitigation measures and warning schemes. The risk analysis for S303 is based on the following assumptions:

(1) The slope stability is evaluated using an infinite slope model. The unsaturated soil shear strength is considered and the pore water pressure in the slope is obtained via infiltration analysis. The analysis procedure and parameters are described in Zhang et al. (2012) and Chen et al. (2015).
(2) The runout of the landslide debris on the mountain terrain is along the steepest direction and governed by an empirical runout model (Chen et al. 2015).
(3) The vulnerability given that a landslide buries the road, $V_{(D:T)}$, is taken as 1.0 considering that vehicles will be completely buried; namely, the passengers will be buried once a landslide runs over them (AGS, 2000). Otherwise, $V_{(D:T)}$ is taken as 0.
(4) The road passengers are regarded as the only element at risk. Assuming a constant traffic flow over the road segment concerned, the expected number of passengers at risk in a landslide event is estimated as 35 persons/km, given by the design vehicle speed (40 km/h), the number of passengers in each vehicle (2.35) and the number of vehicle per hour.

4.1 Ranking the risks of landslide soil deposits

The risks of all 305 landslide deposits on the steep terrain shown in Figure 4 are evaluated and ranked in terms of PLL. The top 25 high-risk deposits are shown in Figure 9, with 1 being the highest risk and vice versa for 25. Many high-risk deposits are hanging at high elevations, from a few hundred meters to 2000 m above the highway, hence cannot be removed or stabilized. The original highway route was therefore at high risk.

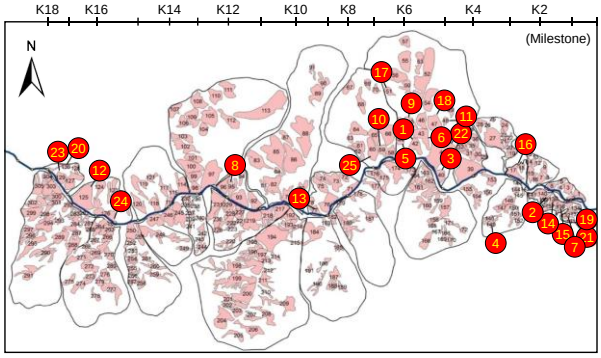

Figure 9. Ranking of landslide soil deposits on steep terrain in terms of potential loss of life.

4.2 Risk profile of the 2009 alignment of S303

Six rainfall scenarios are considered, namely light rain (5mm/12h), moderate rain (15mm/12h), heavy rain (30mm/12h), torrential rain (70mm/12h), large storm (140mm/12h) and extreme storm (240mm/12h), with annual probabilities of 1, 1, 0.7826, 0.2842, 0.0517 and 0.006175, respectively.

The risks of the original highway alignment between K1 and K18 are evaluated and the F-N curves for the landslides that may be triggered by rainstorms of six

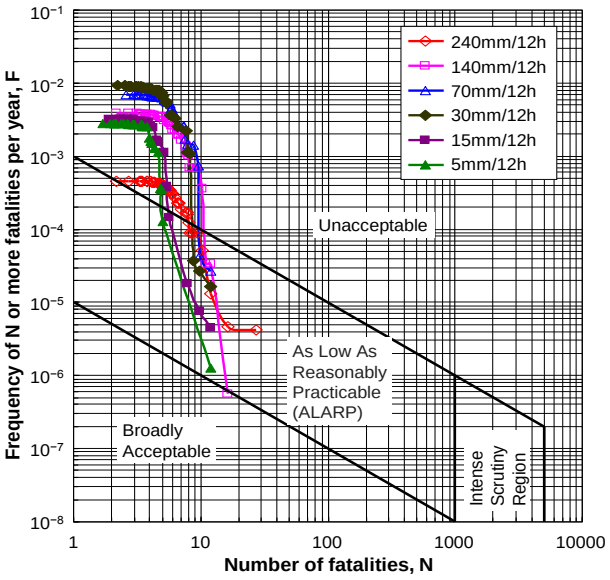

Figure 10. F-N curves for K1-K18 shortly after the earthquake in six rainfall scenarios.

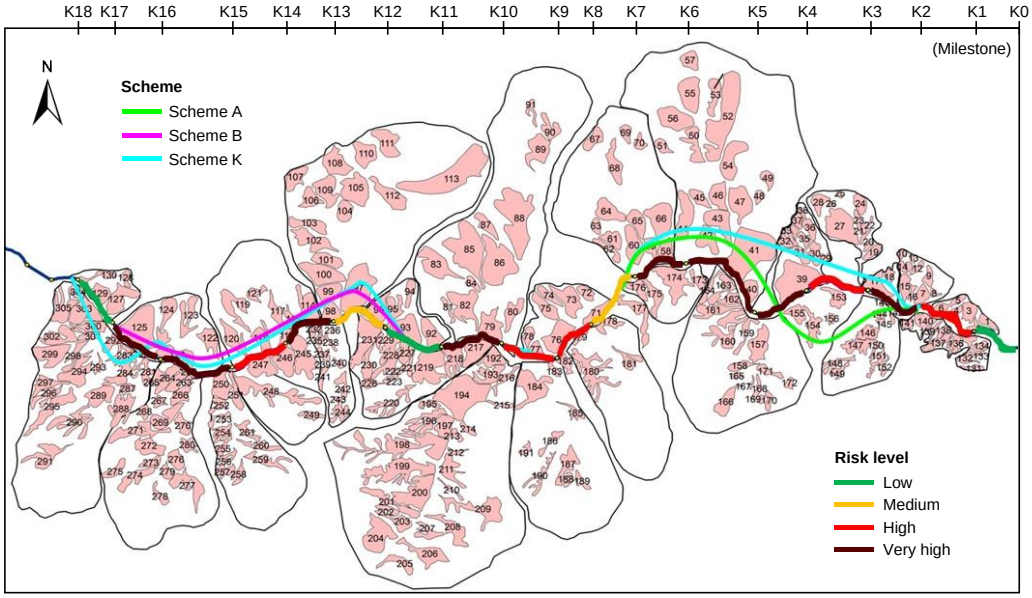

Figure 11. Evaluation of risks of road sections and alternative alignments.

intensities are shown in Figure 10. Based on the tolerance criteria adopted in Hong Kong, the risk levels are very high. This is of course not surprising as the new highway that was nearly completed was destroyed again and again by the rain-induced landslides in 2010, 2011 and 2013. The F-N curves provide a more objective measure to indicate the safety on the highway than does the design factor of safety. Figure 11 further illustrates four levels of risk along the highway. The high-risk road sections are in red and brown, including K2-K7 and K13-K17.

4.3 Effectiveness of risk mitigation measures

In the 2009 reconstruction round, several engineering measures were taken following the design standards of that time, including removing 21 accessible soil deposits, installing flexible barriers at five road sections, and constructing two shed tunnels to protect the open road from rockfall. The effects of these measures can also be quantified using individual risk (Figure 12). Sadly, the clearing and protection measures only lightly lowered the risk level, as evidenced in the reactivation of hanging soil deposits and failure of barriers upon impact.

4.4 Risk profiles of alternative alignments for S303

Given the high risks associated with the 2009 route, three alternative routes adopting tunnels to bypass high-risk zones were considered, as shown in Figure 11, namely, Scheme A to bypass K2-K7, Scheme B to bypass K13-K17, and Scheme K to bypass both. The risks of the alternative alignments are compared quantitatively as well.

Scheme K, which utilizes 5 long tunnels with a total length of 12.5 km to bypass the high-risk areas in the first 18 km, significantly reduced the risk level to about 20% of the initial risk level (Figures 12, 13 and 14). On the F-N curves, the residual risk after adopting the long tunnel plan is slightly above the tolerable level, largely due to the remaining 5.5 km of open road. The individual risk has been well controlled under 10^{-3}, only slightly higher than the tolerable level of 10^{-4} (Figure 14). The presence of residual risks highlights the need to contain risks via monitoring, early warning or other means. Dr. Lacasse rightly pointed out the need to 'learn to live with geohazards" (Lacasse and Nadim, 2011).

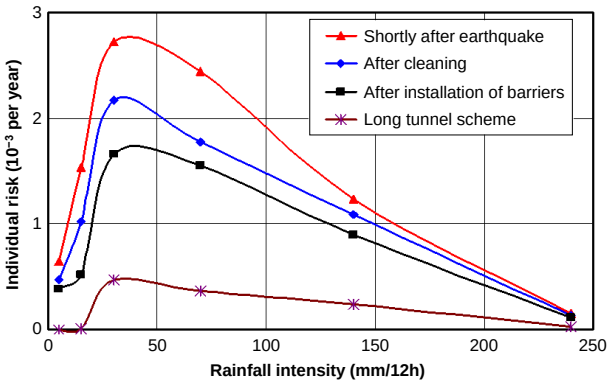

Figure 12. Quantitative description of the effectiveness of landslide risk mitigation measures.

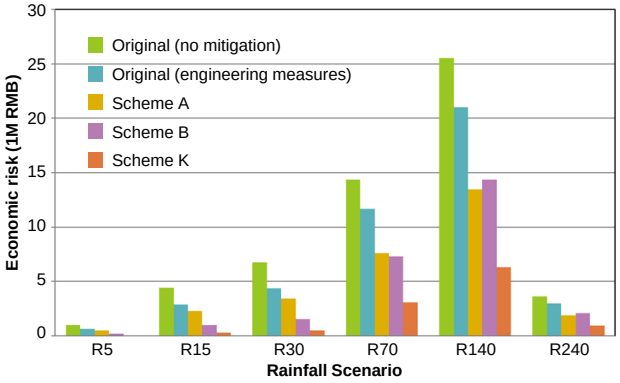

Figure 13. Comparison of economic risk of highway between K1 and K18.

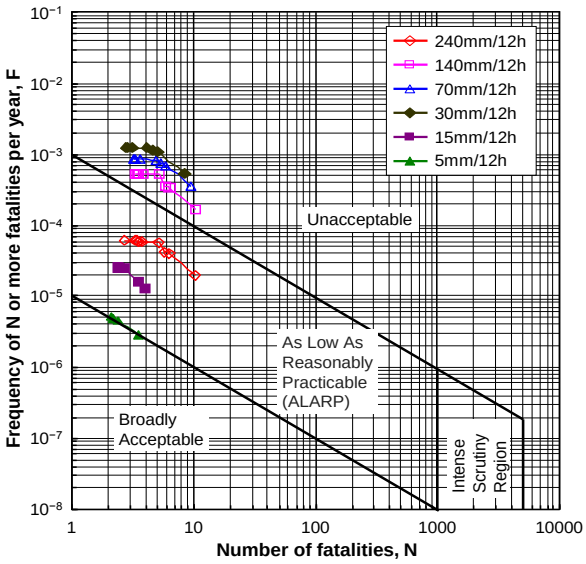

Figure 14. F-N curves for K1-K18 after adopting the long-tunnel scheme (Scheme K).

5. Risk Assessment for G213

Fan (2020) compiled an inventory of co-seismic and post-earthquake landslides and debris flows along G213, as well as their damages to G213 during the period 2008-2020. A comprehensive risk assessment was also performed for the reconstruction of G213.

Take the Gaojiagou-Chediguan section as an example, as shown in Figure 15. The lithology in this area mainly consists of granite. The previous highway (2008 route) is along the Minjiang River. The 2009 new alignment goes across the river and bypasses the Chediguan gully via a tunnel. However, many large-scale landslides and debris flows repeatedly occurred in this section for six out of ten years in 2010, 2011, 2012, 2016, 2019 and 2020. For example, Figure 15 shows the distributions of large-scale debris flows after the 1-3 July 2011 rainstorm. The debris flows largely blocked the Minjiang River at the Gaojiagou gully mouth. The majority of G213 in this section was buried or inundated. If debris flows had also broken in the Luoquanwan gully opposite Gaojiagou, the damage would have been even worse. The 2009 route was reconstructed in a short time, but was repeatedly damaged in 2010, 2011 and 2013. Finally, a new route was redesigned in 2015, which adopts a 5 km long tunnel (Futang Tunnel) to bypass all landslide-prone areas from Gaojiagou to Chediguan through experiences learned from the reconstruction of S303. The latest 2015 route was completed in December 2018.

An integrated multi-hazard analysis software, EDDA 2.0 (Shen et al., 2018), was applied to simulate the rain-induced landslides and debris flows in this area and evaluate the risks of three possible highway alignments (i.e. 2008, 2009 and 2015 routes). Figure 16 shows the deposition depths under the August 2010 rainstorm. The maximum depth exceeds 20 m, resulting from the merging of two debris flows from Gaojiagou and Luoquanwan. The 2008 and 2009 open routes will be significantly affected by such severe hazard.

Figure 15. Debris flows on 3 July 2011 rainstorm, which largely blocked the Minjiang River and damaged G213.

The risks to passengers are further assessed for the three schemes. Table 1 compares the potential loss of life associated with each scheme. The 2009 scheme inadequately considered long-term landslide activities and was at high risk. The 2015 long-tunnel scheme bypasses three debris flow gullies and mitigates more than two thirds of the estimated loss of life risk.

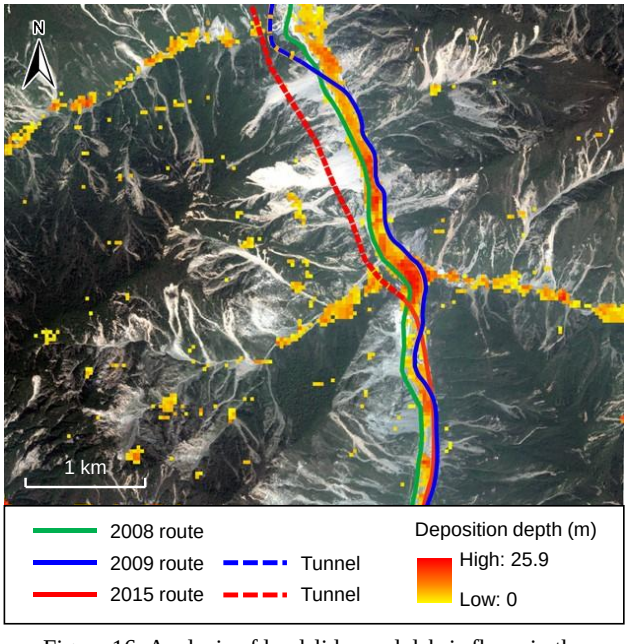

Figure 16. Analysis of landslides and debris flows in the Gaojiagou-Chediguan section under the August 2010 rainstorm.

Table 1. Potential loss of life in three highway schemes of G213 under the August 2010 rainstorm.

Highway route	2008 route before earthquake	2009 reconstruction route	2015 tunnel scheme
PLL	23.1	33.6	8.9

Figure 17 shows the final 2015 route for G213 in the study area. Four long tunnels are adopted to bypass the major landslide and debris flow gullies in the section between Yingxiu and Dayiping, significantly decreasing the landslide risks. It should be noted that residual risks remain, arising from landslide risks at open sections, bridge locations and tunnel portals.

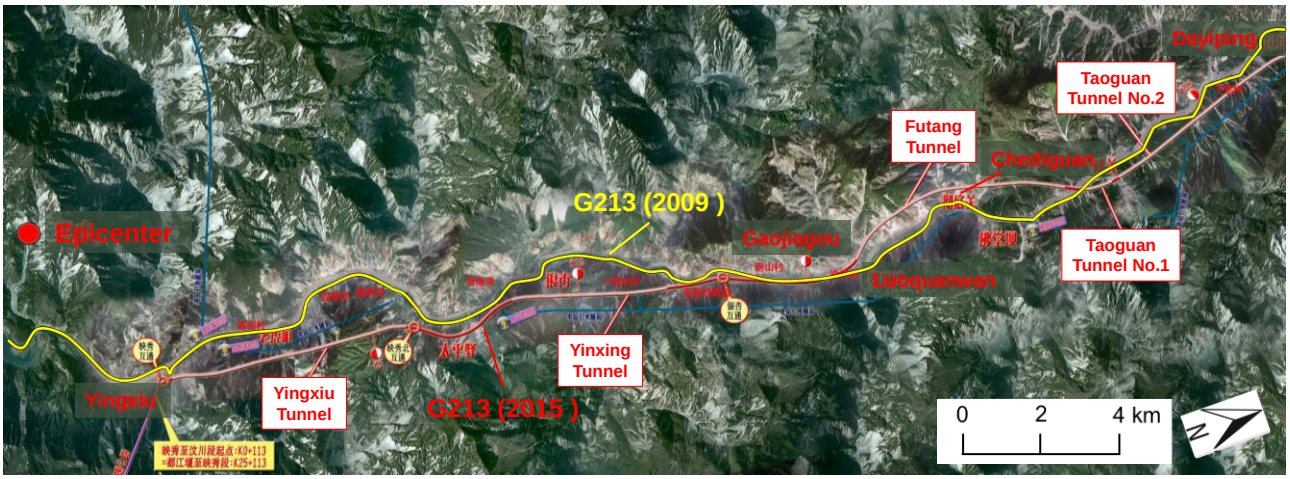

Figure 17. The 2015 alignment for G213 that adopts long tunnels to bypass active landslide and debris flow zones.

6. Summary and Conclusions

This paper describes the important role that quantitative risk analysis played in the reconstruction of two mountain highways, S303 and G213, over a period of 10 years in the epicentral area of the 2008 Wenchuan earthquake.

The highways were damaged during the earthquake in May 2008, and early stage reconstruction works faced life-threatening landslide hazard chains in the forms of rock falls, rain-induced landslides, debris flows, landslide damming and flooding. The traditional factor of safety design approach did not adequately assess the safety of the highways and the effectiveness of proposed risk mitigation measures, leading to another round of reconstruction. In contrast, the implementation of systematic highway risk management in the final round of reconstruction led to reasonably safe highways, and the reconstruction of S303 and G213 was successfully completed in Oct. 2016 and Dec. 2018, respectively.

This paper presents risk-informed decisions in selecting the highway alignments and engineering risk mitigation measures. A quantitative risk assessment procedure was followed to assess the landslide risks for each alignment option, and for proposed engineering risk mitigation measures. Great efforts were made to understand the landslide hazard chains along the highways, the interactions among the separate hazards in each chain, and their evolution over time. The quantitative risk assessment led to the use of long tunnels to bypass the high-risk zones and the use of other engineering risk mitigation measures to cope with manageable, smaller scale hazards in the final round of reconstruction of these two highways. A decade later, this method has become routine practice in the design and construction of new highways in the seismic mountainous region of western China.

Acknowledgements

The authors are grateful to many individuals who provided technical advice and encouragements in the course of the research reported in this paper. We benefited tremendously from Dr. Suzanne Lacasse's insight regarding landslide risk communications and holistic risk management. We enjoyed a decade-long technical communication on S303 and G213 with Messrs. Bo Xiang, Changfeng Yang and Weilin Zhuang of the Sichuan Highway Planning, Survey, Design and Research Institute Ltd. Seven PhD students at the Hong Kong University of Science and Technology, namely Drs. Shuai Zhang, Hongfen Zhao, Hongxin Chen, Dongsheng Chang, Ping Shen, Ming Peng and Ruilin Fan, worked on the earthquake-induced landslide subject. Miss Melissa Zhang of Stanford University proof read the manuscript.

The work described in this paper was substantially supported by Sichuan Department of Transportation and Communications, the National Science Foundation of China (Grant No. 41941017), and the Research Grants Council of the Hong Kong SAR (Grants No. 16206217 and C6012-15G).

References

Australian Geomechanics Society (AGS), Committee on Landslide Risk Management. 2000. Landslide risk management concepts and guidelines. *Australian Geomechanics*, 35(1): 49–92.

Chen, H.X., Zhang, L.M., Chang, D.S. and Zhang, S. 2012. Mechanisms and runout characteristics of the rainfall-triggered debris flow in Xiaojiagou in Sichuan Province, China. *Natural Hazards*, 62(3): 1037–1057.

Chen, H.X. and Zhang, L.M. 2014. A physically-based distributed cell model for predicting regional

rainfall-induced slope failures. *Engineering Geology*, 176: 79–92.

Chen, H. X., Zhang, L. M., Gao, L., Zhu, H. and Zhang, S. 2015. Presenting regional shallow landslide movement on three-dimensional digital terrain. *Engineering Geology*, 195: 122–134.

Chen, H.X. and Zhang, L.M. 2015. EDDA 1.0: integrated simulation of debris flow erosion, deposition and property changes. *Geoscientific Model Development*, 8: 829–844.

Fan, R.L., Zhang, L.M., Wang, H.J. and Fan, X.M. 2018. Evolution of debris flow activities in Gaojiagou Ravine during 2008–2016 after the Wenchuan earthquake. *Engineering Geology*, 235: 1–10.

Fan, R.L. 2020. Long-term evolution of post-earthquake landslides and debris flows in the epicentral area of the 2008 Wenchuan earthquake. *Ph.D. Thesis*. The Hong Kong University of Science and Technology, Hong Kong.

Fan, X., Scaringi, G., Korup, O., van Westen, C., Tanyas, H., Hovius, N., Hales, T.C., Jibson, R.W., Allstadt, K.E., Zhang, L.M., Evans, S., Xu, C., Li, G., Pei, X.J., Xu, Q. and Huang, R.Q. 2019. Earthquake-induced chains of geologic hazards: Patterns, mechanisms, and impacts. *Reviews of Geophysics*, 57(2): 421–503.

Fell, R., Ho, K.K., Lacasse, S. and Leroi, E. 2005. A framework for landslide risk assessment and management. In *Landslide Risk Management*, Edited by Hungr, O. et al. Taylor & Francis Group, London, UK, pp. 3–25.

Huang, R. and Fan, X. 2013. The landslide story. *Nature Geoscience*, 6(5): 325–326.

Lacasse, S. and Nadim, F. 2009. Landslide risk assessment and mitigation strategy. In *Landslides–Disaster Risk Reduction*, Edited by Sassa K., Canuti P. Springer, Berlin, Heidelberg, pp. 31–61.

Lacasse, S. and Nadim, F. 2011. Learning to live with geohazards: From research to practice. In *GeoRisk 2011: Geotechnical Risk Assessment and Management (GSP 224)*, Edited by Juang, C.H. et al. ASCE, Reston, pp. 64–116.

Shen, P., Zhang, L.M., Chen, H.X. and Fan, R.L. 2018. EDDA 2.0: integrated simulation of debris flow initiation and dynamics considering two initiation mechanisms. *Geoscientific Model Development*, 11(7): 2841–2856.

Zhang, L.M., Zhang, S. and Huang, R.Q. 2014a. Multi-hazard scenarios and consequences in Beichuan, China: the first five years after the 2008 Wenchuan earthquake. *Engineering Geology*, 180: 4–20.

Zhang, S. 2014. Assessment of human risks posed by cascading landslides in the Wenchuan earthquake area. *Ph.D. Thesis*. The Hong Kong University of Science and Technology, Hong Kong.

Zhang, S. and Zhang, L.M. 2017. Impact of the 2008 Wenchuan earthquake in China on subsequent long-term debris flow activities in the epicentral area. *Geomorphology*, 276(1): 86–103.

Zhang, S., Zhang, L.M. and Glade, T. 2014b. Characteristics of earthquake- and rain-induced landslides near the epicentre of Wenchuan Earthquake. *Engineering Geology*, 175: 58–73.

Zhang, S., Zhang, L.M., Nadim, F. and Lacasse, S. 2016. Evolution of mass movements near epicentre of Wenchuan earthquake, the first eight years. *Scientific Reports*, 6: 36154.

Zhang, S., Zhang, L.M., Peng, M., Zhang, L.L., Zhao, H.F. and Chen, H.X. 2012. Assessment of risks of loose landslide deposits formed by the 2008 Wenchuan earthquake. *Natural Hazards and Earth System Sciences*, 12: 1381–1392.